AE-208
UDC 539.125.523.5

AE-208

Measurement of the Neutron Slowing-Down Time Distribution at 1.46 eV and its Space Dependence in Water

E. Möller

AKTIEBOLAGET ATOMENERGI
STOCKHOLM, SWEDEN 1965

MEASUREMENT OF THE NEUTRON SLOWING-DOWN TIME DISTRIBUTION AT 1.46 eV AND ITS SPACE DEPENDENCE IN WATER

E. Möller

Summary

The use of the time dependent reaction rate method for the measurement of neutron slowing-down time distributions in hydrogen has been analyzed and applied to the case of slowing down in water. Neutrons with energies of about 1 MeV were slowed down, and the time-dependent neutron density at 1.46 eV and its space dependence was measured with a time resolution of 0.042 μs. The results confirm the wellknown theory for time-dependent slowing down in hydrogen. The space dependence of the distributions is well described by the P_1-calculations by Claesson.

Printed and distributed in December 1965.

LIST OF CONTENTS

1. Introduction

The time dependence of the slowing-down to the eV region of neutrons in water has been the object of few detailed experiment studies. The theory of the process is well known in the idealized case of a homogeneously distributed pulsed source in hydrogen gas of infinite dimensions, and attempts to treat the problem in more realistic cases have also been made. The knowledge of the space-, time- and energy-dependent slowing-down flux in hydrogeneous media is of interest since slowing down preceds the thermalization, the time dependence of which can also be studied experimentally and be compared with predictions, based on the scattering laws for different models of the scattering process. The mastering of the time-dependent slowing-down process is also important for the production of short pulses of moderated neutrons by means of accelerators.

2. Earlier work on the time-dependence of slowing-down

a) Theory

The theory of the slowing-down of neutrons from a distributed pulsed source in hydrogen has been given by Ornstein and Uhlenbeck [1] and Marshak [2]. They expressed the velocity- and time-dependent neutron density $n(v,t)$ for velocities v much smaller than the source velocities in the following way:

$$n(v,t) = v\Sigma_s{}^2 t^2 \, e^{-v\Sigma_s t} \qquad (1)$$

where Σ_s is the macroscopic cross section for scattering, assumed to be constant, an assumption which is approximately fulfilled in the energy region $1 - 10^4$ eV. The absorption, leading to an exponential decay of the spectrum, has been neglected. The maximum density of neutrons of a chosen velocity v' occurs at a time $t_{max.n}$.

$$t_{max.n} = \frac{2}{v'\Sigma_s} \qquad (2)$$

Another important entity is the time-dependent slowing down density $q(v',t)$, for which the following relation may be obtained:

$$q(v', t) = \frac{d}{dt} \int_0^{v'} n(v, t)\, dv = v'^2 \Sigma_s^2 t\, e^{-v'\Sigma_s t} \tag{3}$$

with a maximum at

$$t_{max.q} = \frac{1}{v'\Sigma_s} \tag{4}$$

The mean slowing-down time $\bar{t}$ to the neutron velocity v' is given by the following expression:

$$\bar{t} = \frac{\int_0^{\infty} t \cdot q(v', t)dt}{\int_0^{\infty} q(v', t)dt} \tag{5}$$

In the case that the Eq. (3) can be used for the slowing-down density, the slowing-down time will be:

$$\bar{t} = \frac{2}{v'\Sigma_s} \tag{6}$$

In water Σ_s equals $1.33\ cm^{-1}$, assuming a scattering cross section of 20 barns for hydrogen. The values of $\bar{t}$ (or $t_{max.n}$) calculated from (6) is then 0.90 μs at $E' = 1.46$ eV. Extending the calculation to lower energies, one obtaines 1.54 μs for 0.5 eV and 1.84 μs for 0.35 eV.

The actual deviation of the hydrogen cross section from a constant value of 20 barns, especially at higher energies, will extend the time scale somewhat when the neutrons start from energies in the MeV range, but this effect is quite small since the last collisions play dominant role for the establishment of the time distribution. The increase of the mean free path with energy is much more important for the spatial distribution. The presence of oxygen will speed up the slowing down somewhat, but the cross section as well as the energy transfer per collision are quite small. The thermal motion of the moderator atoms will prolong the slowing down process, but above 1 eV the effect is very small. The slowing down time to 1.46 eV, calculated from Eq. (6), can thus be estimated to be correct to within a few per cent, and the distributions given by Eqs. (1) and (3) should not be much distorted by the three effects mentioned above.

The experimental study of time-dependent spectra implies the use of a pulsed point source, which means that the space dependence, i.e. the effects of the diffusion during the moderation, must also be taken into account. Theoretical work on this problem has been done by Dyad'kin and Batalina [3] and Claesson [4]. In the former work, the general case of a mixture of different nuclei has been treated and expressions for $n(r,v,t)$ and $t_{max.n}$ are given. Claesson [4] calculated $n(r,v,t)$ and $t_{max.n}$ in a P_1-approximation for the case of hydrogen gas. The results are also given in diagrams for the velocity corresponding to the energy 1.46 eV of the indium resonance.

Von Dardel [5] treated the time dependence of the neutron flux during both slowing-down and thermalization in his pioneering work on the use of a pulsed neutron source for the study of the energy spectrum as a function of time. The change from a slowing-down process taking place by neutron collisions with protons at rest into a thermalization by neutron interactions with molecules or with a proton gas was also studied by means of the Monte Carlo method.

A more detailed Monte Carlo calculation of the distribution of slowing-down times to 0.35 eV was performed by Haynam and Crouch [6]. The resulting distribution shows a peak around 1 μs after the start of the fast neutrons. The time value for the maximum slowing-down density at 0.35 eV, calculated from eq. (4) using $\Sigma_s = 1.33\ cm^{-1}$ is 0.92 μs. Since the neutron histories followed were only 1000, the statistical fluctuations became quite large and no conclusions about the detailed shape of the distribution could be drawn. The value of the slowing-down time obtained was 0.85 μs for 1.4 eV and 1.7 μs for 0.35 eV. The possible influence of the presence of oxygen and the chemical binding effects were not investigated.

Krieger and Federighi [7] solved the time-dependent Boltzmann equation by Laplace transformation, for which the time variable can be treated as a fictitious absorption term [8]. A numerical inversion was performed using scattering cross sections from two different water models and the slowing-down density integrated. A slowing down time for the energy 0.35 eV of 1.6 μs was found.

The understanding of the time-dependent slowing-down in a small geometry is of considerable importance for the efficient production of

short bursts of moderated neutron. Michaudon [9] applied the Monte Carlo method of calculation for various geometries and derived a figure of merit for each.

b) Experiments

The first experimental investigation of the time scale of neutron slowing-down in hydrogenous substances was performed by von Dardel [5], using a pulsed source for measurements on both light and heavy water. The transmission of neutrons from the moderator assembly through boron and cadmium absorbers was measured as a function of time. Agreement with the theory was obtained within the experimental accuracy. However, since the time resolution was, at that time, limited to about 2 μs, the slowing down process could not be studied in detail. An uncertainty was also inherent in the time-of-flight corrections.

Crouch [10] measured the distribution of slowing-down times to 0.35 eV in water. A Po-Be-source was used as a "pulsed" source. The instant of neutron production could be found by the detection of the simultaneously emitted gamma rays. After being slowed down, the neutrons were detected by means of a boron counter, used with a cadmium difference technique in order to yield energy selective information. The measured mean slowing-down time to 0.35 eV was 5.2 μs. This is considerably larger than the value calculated by the use of the free proton model. The difference seems to be too great to be explained by chemical binding effects and was probably caused by time-of-flight effects in the detector [11].

The indirect neutron detection by the recording of gamma rays from neutron capture can be done with a very good time resolution. This method was used by Engelmann [12, 13] in a study of the neutron slowing-down in a small geometry of lead acetate, a substance chosen for its low proton density and thus extended time scale. The injected neutron bursts had a duration of about 1 μs. An indium foil, shielded from thermal neutrons, was placed in the moderator, and gamma rays from neutron capture in the resonance at 1.46 eV were detected by means of a plastic scintillator. The time distribution of the detector pulses was recorded photographically from an oscilloscope. The experimental conditions made it difficult to obtain good statistical accu-

racy, and the effects of the position and the thickness of the foil were not investigated. However, the experiment supports the validity of Eq. (1), even if it could not be verified in details.

Möller and Sjöstrand [14, 15, 16] applied the method of time analysis of capture gamma rays from the reaction between the flux and a spectrum indicator by dissolving the neutron capturing substance in small quantities. The flux perturbation could, in this way, be decreased, and effects of time-dependent flux depression, which are difficult to analyse, could be reduced. These studies gave integral information about the time dependence of the thermalization, but from the measurements a slowing down time to 0.2 eV of 2.7 μs was also obtained. The free proton model yields a time of 2.42 μs, within the error of the experiment, indicating that predictions from the free proton scattering model are, at this energy, not yet seriously wrong, although the chemical binding becomes important in this energy region.

Experiments based on the detection and time analysis of capture gamma rays have also been performed by Shukla and Waltner [17] using an Am-Be neutron source and Profio and Eckard [18], who used a 150 kV neutron generator. The quantitative information obtained in these experiments is rather limited because of low source intensities, unknown influence of the small geometries used, and the perturbation of flux and time spectrum caused by the heavy loading of the moderator by spectrum indicators as foils and in solution.

Information about the slowing down time may also be obtained by measurements of the cadmium ratio of the flux in a moderator from a stationary source, based on the principle that the reaction of the flux of a certain energy with a 1/v-detector is proportional to the life-time of neutrons of that energy. DeJuren [19] found a slowing down time to 0.5 eV of 1.54 μs. Grosshög [20] improved the method and also used a gadolinium filter for measurements at 0.3 eV. The resulting slowing down time values are 1.60 ± 0.07 μs for 0.5 eV and 2.47 ± 0.11 μs for 0.3 eV.

Most parameters obtained in the experiments reviewed for the description of the time-dependence of neutron slowing-down are in agreement with the theoretically predicted ones, but the accuracy of the measurements has not been sufficient to allow for a detailed comparison with

the theoretical expressions for the number density or slowing-down density. No measurements have been made of the space dependence of these quantities. The experimental limitations are low neutron source strengths, insufficient time resolution and lack of analysis of the distortions caused by the methods for energy selective neutron detection. It was therefore found worthwhile to make experiments under improved experimental conditions and with the aim to compare the results with theories, which include the effects of diffusion during the moderation.

3. Principles of the experiment

The present investigation has been undertaken with the aim of measuring the time- and velocity-dependent neutron density and its space dependence in water in the energy region for slowing-down in order to get an experimentel confirmation of the theoretical expression $n(v,t)$ given by Marshak [2] and also to see how well the spatial dependence of the distribution is described by current theories. The method developed for our earlier work on the time-dependent thermalization has been used. A short burst of neutrons is produced in the moderator. The time-dependent reaction rate from the interaction of the flux with a spectrum indicator is recorded by time analysis of prompt gamma rays emitted in the neutron capture. The spectrum indicator is distributed by dissolving it in the water. The recorded reaction rate $R(t)$ is given by the following equation:

$$R(t) = \int \Phi (E,t)\, \Sigma_a (E) dE \qquad (7)$$

In order to record $\Phi(E,t)$ for a selected energy, which is equivalent to the measuring of $n(v,t)$, the cross section of the indicator should be zero at all energies except for the selected one. In practice, one must use elements with a more or less sharp capture resonance, which have also a finite cross section at other energies. There are several elements with such isolated resonances in the lower eV region, such as rhodium (1.26 eV), indium (1.46 eV), silver (5.20 ev) and gold 4.91 eV). Indium was chosen for this work since it is generally used for flux mapping and connection to stationary measurements would be possible if desired. Indium has other resonances in this region, of

which the most important occur at the energies 3.86 and 9.10 eV. These will also contribute to the reaction rate curve, but this can be corrected for. Neglecting the higher resonances, the indium cross-section in BNL-325 [21] may be described as a resonance at 1.47 eV with a peak cross-section value of 28400 barns and with a width of 0.086 eV [22]. At lower energies, the cross section changes into the 1/v-type as prescribed by the Breit-Wigner formula, and at 0.025 eV the cross-section value is 194 barns.

It is necessary to examine carefully the effect of the presence of the indicator in the water. The recorded time-dependent reaction rate will give an incorrect picture of $n(r, v, t)$ for the pure moderator if the concentration is high. There are two reasons for this. One is the introduction of a flux depression at the energy of the resonance. The other is a distortion with a time shift of the curve. Both perturbations increase with concentration.

The perturbation of a stationary neutron spectrum near a resonance at the energy E is well known and treated in textbooks on neutron physics. For our purpose, we can use the resonance escape probability as a measure of the perturbation. For hydrogen it is given by

$$p(E) = e^{-\int_{E}^{E_o} \frac{\Sigma_a}{\Sigma_a + \Sigma_s} \frac{dE'}{E'}} \qquad (8)$$

E_o is the energy of the source neutrons, Σ_s and Σ_a are the (energy dependent) macroscopic cross sections for scattering and absorption. If $p(E)$ were evaluated for the indium resonance with $E \sim 1$ eV and found to be 0.95, for example, one should expect the distortion of the reaction rate curve to be small at a later time when all the neutrons had surpassed the resonance. Five per cent of the neutrons would be lost, but the effect on the spectrum shape would be very small, since these neutrons would, if they had not been captured, have been distributed evenly over the whole energy region. The asymptotic reaction rate would, in the case of an infinite medium, in the first approximation be proportional to the neutron density multiplied by $p(E)$ and Westcott's g-factor [22]. If the measurement is done in a large moderator geometry with a small indicator container, the diffusion at the boundaries of the container will reduce the flux perturbation. A quan-

titative analysis will then be difficult, since the exchange of neutrons between the two regions depends on the shape and size of the container and the spatial distribution of the neutrons.

The effect of time-shift of the curve is more serious and does not seem to have been considered earlier. If a measurement is made with a thick foil of indium, it will absorb all the neutrons in the surroundings with the energy of the resonance, and also many of the slower ones, as soon as they slow down into that region. The recorded curve will not show the neutron density but something more like the time-dependent slowing down density, followed by the rate of diffusion into the foil position. The maximum of the recorded curve will be shifted towards shorter times as seen by comparing the expressions for $t_{max.q}$ and $t_{max.n}$. If on the other hand the measurement is made with a solution of the indicator with an absorption cross section Σ_a at the velocity v' of the resonance, a neutron scattered down into this velocity region will not disappear from it with a decay constant $v' \Sigma_s$ as assumed in the theory for the purely scattering moderator. It will have an effective decay constant $v'(\Sigma_s + \Sigma_a)$ and thus contribute to the neutron density during a shorter time. The mean time for detection (i.e. absorption) will occur at an earlier time than predicted by Eq. (1).

The effect can be analyzed by considering the neutron balance at the velocity v'. The neutrons are fed down into the velocity interval by a source $S(v',t)$.

$$\frac{\partial n(v',t)}{\partial t} = S(v',t) - v'(\Sigma_s + \Sigma_a)\, n(v',t) \tag{9}$$

For $\Sigma_a = 0$ the solution is given by Eq. (1), and we find by inserting $n(v,t)$, Eq. (1), in Eq. (9)

$$S(v',t) = 2v'\Sigma_s^{\,2} t\, e^{-v'\Sigma_s t} \tag{10}$$

Using this source, we find the solution of Eq. (9) for the case of non-zero-absorption at the velocity v' to be

$$n(v',t) = \frac{2\Sigma_s^{\,2}}{v'\Sigma_a^{\,2}}\, e^{-v'\Sigma_s t}\left(v'\Sigma_a t - 1 + e^{-v'\Sigma_a t}\right) \tag{11}$$

For weak absorption, Eq. (11) can be written as

$$n(v',t) = v'\Sigma_s{}^2 t^2 e^{-v'\Sigma_s t} \left(1 - \frac{1}{3}v'\Sigma_a t + \frac{1}{12}(v'\Sigma_a t)^2 - \frac{1}{60}(v'\Sigma_a t)^3 + \ldots\right) \quad (12)$$

The quantity that is measured is directly proportional to $n(v',t)$ as given by Eq. (11), so we see, that the recorded curve will deviate from the unperturbed neutron density. It is thus important, when measuring the time-dependent neutron density by our method, to keep the concentrations low and to correct for the unvoidable curve distortion. In case the indicator is dissolved in a container, the time-shift effect is also reduced by the diffusion at the boundaries, since neutrons of resonance energy have a longer lifetime outside the container and may diffuse into it at a later time.

4. The performance of the experiment

The experiment was performed under essentially the same conditions as the earlier thermalization studies [16]. The water, 1 m^3, was poisoned with boric acid to a neutron lifetime of 60 μs in order to reduce the overlap between succeding cycles. The duration of the neutron burst was set at 0.04 μs by adjustment of the terminal pulser of the van de Graaff accelerator, and the pulse separation was 250 μs except for a few runs with 100 μs. Indium sulphate was used for the indium solutions, and to these were also appropriate amounts of boric acid added in order to obtain the same lifetime in the indicator containers as around them. Two types of plastic pots were used as containers. The larger was slightly conical and had a volume of 1.5 l with a smallest and largest diameter of 11.0 and 13.6 cm respectively and a height of 14.0 cm. The smaller pot was cylindrical with a volume of 0.4 l, a diameter of 11.5 cm and a height of 4.0 cm. It was used to yield a finer spatial resolution near the source. In this case, the pot was used with its bottom facing the source. The geometrical conditions are illustrated in Fig. 1. The container distance from the lithium target in the center of the water could be changed, and the plastic scintillation detector was kept in the same position over the container as its position was changed. Measurements were also made with a very dilute indium sulphate solution in the whole tank and with the detector at a distance of 12 cm from the source. The time analysis was made by means of a time-to-pulse height converter and a pulse height analyser. The time analyser was started before the

time of the neutron burst, and channel widths of 0.0417, 0.0834, and 0.313 μs were used. The proton energy was 3.7 MeV, which means that the fast neutrons from the lithium target had energies up to 2 MeV.

The measurements with the containers were made with three different concentrations. This would make it possible to estimate the degree of distortion of the curves. The contribution from indium to the macroscopic absorption cross section at 1.46 eV was 7.88 cm^{-1}, 0.788 cm^{-1} and 0.237 cm^{-1} respectively. The corresponding resonance escape probabilities are 0.92, 0.96 and 0.98. The change of the effective lifetime in the medium for a neutron of the energy 1.46 eV would be 0.39, 0.17 and 0.07 μs respectively. For each concentration, records were taken at several distances. The measurements were corrected for the dead time of the analyser. The overlapping background and the normalized background run without the indicator pot were subtracted. The decay constant for the overlapping background was determined in separate measurements.

5. Results of the measurements

Fig. 2 shows the curves measured with a channel width of 0.0417 μs at a distance of 3 cm between the source and the container with the concentration II. The dead time correction has been performed. The neutrons were injected at channel number 45. The indium curve shows a rise in the reaction with maximum occurring at channel 65 approximately. This corresponds to 0.83 μs. Then the reaction rate decreases and has reached an asymptotoc level at channel number 190, corresponding to 6 μs after injection. From there on, the reaction rate decreases due to the leakage and the absorption of the neutrons in hydrogen, boron and indium in the water. The background curve (experimental points replaced by a solid line) would be expected to show a decay from the moment of injection since now the capture should take place only in the hydrogen of the water. The smooth rise actually observed during the first microseconds depends on a contributing reaction with the material of the detector, probably capture in chlorine, which was present in the black tape used for light shielding of the detector and light pipe. It has a negative resonance, causing a rise in the cross section at lower energies.

Fig. 3 shows curves, with background subtracted, for the three concentrations measured with a source-container distance of 3 cm. They have been vertically displaced in order to avoid mixing of the points. The curve for the highest concentration is at the top and for the lowest at the bottom. All curves have been normalized to the same peak value. We see, that with increase of the concentration, the peak is shifted to shorter times. The shape of the curves is also changed. The full line curve included in the figure is a predicted curve calculated for the infinite medium case and for no perturbation of the indicator as will be described in the next section.

In Fig. 4 the results of the measurements with the weakest solution are shown. The measurements for the container-source distances x = 7.0, 11.0 and 13.0 cm (a) were made with the big container and a time resolution of 0.0834 μs, whereas the measurements closer to the source (b) were made with the small container and a time resolution of 0.0417 μs. The two sets of curves are normalized within themselves but not relative to each other. The curve at x = 13.0 has been lowered in the figure.

The measurement with indium in the whole tank resulted in a curve which is, except for a slight shift towards longer times, identical with the one shown for x = 5.5 cm. Measurements were also made with the higher concentrations at several distances, but since these mainly give further support for the use of weak solutions, they are not shown.

It is clear from Fig. 4, that the maximum of the curves appears at longer times when the distance from the source increases. Before analyzing this effect of diffusion, we must consider what to expect from the measurements for the case of an infinite medium with a homogenously distributed source.

6. Calculated expected curves for the infinite medium case

The experimental curves may be characterized by their shape and the time for the maximum reaction. Before comparing them with theoretical predictions, we need some knowledge about the effect of the finite width of the indium resonance, the contribution from the higher resonances and the magnitude of the time shift caused by the actual indicator concentrations used.

The theoretical reaction rate curve to be expected per indicator atom for the infinite medium case if Eq. (1) is valid, may be calculated by integrating the corresponding flux over the resonances of indium. Describing a resonance by the well-known Breit-Wigner formula

$$\sigma_\gamma(E) = 4\pi\lambda\!\!\!^{-}_o{}^2 g\,\Gamma_n\,\Gamma_\gamma\,E_o^{1/2}E^{-1/2}\left(4(E-E_o)^2+\Gamma^2\right)^{-1} \qquad (13)$$

where the symbols have their usual meaning, we find

$$R(t) = 4\sqrt{2\pi}\left(\frac{c}{m}\right)^{3/2} g\lambda\!\!\!^{-}_o{}^2 E_o^{1/2}\,\Gamma_n\,\Gamma_\gamma\,\Sigma_s{}^2t^2\int_o^\infty e^{-\left(\frac{2c}{m}\right)^{1/2}E^{1/2}\Sigma_s t}$$

$$\left(4(E-E_o)^2+\Gamma^2\right)^{-1}dE \qquad (14)$$

The equation is normalized to unit neutron density. c is the conversion factor from electron volt to erg, and m is the mass of the proton and the neutron.

The formula should be valid as long as Eq. (1) may be assumed to be correct, i.e. down to about 1 eV. However, the calculation may be extended to times, which are so long that the neutrons will have passed this energy and even have become thermal, since when the neutrons pass into the region where the protons are bound, the indium cross section changes into the 1/v-type, and than the equation simply yields the neutron density, independent of the velocity distribution. The asymptotic value of R(t) is found by neglecting E and Γ in comparison with E_o.

$$R(\infty) = \left(\frac{2c}{m}\right)^{1/2}\frac{\pi\lambda\!\!\!^{-}_o{}^2 g\Gamma_n\Gamma}{E_o^{3/2}} \qquad (15)$$

(This property of Eq. (14) is also understood by thinking of the capture cross section as a sum of a sharp peak and a 1/v-part, the contribution from the former vanishing when the neutrons become thermal.) In the intermediate time region, minor errors will arise. The asymptotic value should be corrected for the slight deviation from the 1/v-law. This correction is given by Westcott's g-factor, which for indium is 1.02 at room temperature.

R(t) curves have been calculated for the three resonance of indium which give the main contribution in the time region of interest. The parameters for the 1.46 eV resonance have been taken from Westcott's fit [22] to the experimental cross section in BNL 325 [21], whereas the parameters for the 3.86 and 9.10 eV resonance have been taken from BNL 325. The results are shown in Fig. 5. The peaks appear at the times 0.90, 0.55 and 0.35 μs respectively. The yield of the two higher resonances is rather small compared to the yield from the 1.46 eV resonance.

The asymptotic level has been subtracted from the curve for the 1.46 eV resonance and the resulting curve has been compared with the neutron density curve given by Eq. (1). The two curves agree very well in shape, which means that the measured curves may be relat d to the resonance energy, although a finite energy range has contributed to the reaction rate.

The calculations of the time shift of the curves, caused by the indicator concentrations used, have been made by the use of Eq. (11). Fig. 6 shows the four curves with macroscopic absorption cross sections at the resonance energy from 0 to 7.88 cm^{-1} and with an assumed Σ_s of 1.333 cm^{-1}. The curve to the right is the time-dependent neutron density in the absence of the indicator with its maximum at 0.90 μs. With increasing amounts of indicator, the time distribution is shifted towards shorter times. The peak in the distribution is found at the times 0.85, 0.77 and 0.55 μs for the cross sections 0.237, 0.788 and 7.88 cm^{-1} respectively. The shape of the curves is also changed.

A method to obtain the time for the maximum of the measured curves was checked by least-squares fitting to the calculated curves of Fig. 5 the following function.

$$f(t) = at^2 e^{-bt} + c \qquad (16)$$

which has its maximum at $t_{max} = \frac{2}{b}$. The values of the time of the maximum, as obtained from the fitted parameter b, were 0.85, 0.78 and 0.60 μs. The function of Eq. (16) reproduces the curves, calculated from Eq. (11), very well except for the case with the strongest solution, which is also seen in the discrepancy in the time value. It is

therefore concluded, that the function of Eq. (16) is suitable for use in determining the time of the maximum in the measured curves with an accuracy of 1 % for the weakest solution.

As mentioned earlier, the slowing-down time in water can be expected to deviate slightly from the value calculated for hydrogen gas of corresponding density. The magnitude of the effect was checked by the use of a Monte Carlo program for the computation of energy and space dependent slowing down distributions in water, developed by Högberg, Ljunggren and Persson [23]. A small change in the program resulted in the recording of the time-dependent slowing-down density. The actual scattering cross sections for hydrogen and oxygen were used. 10^5 neutrons were started with an energy of 0.5 MeV and slowed down to 1.5 eV. The slowing-down time, calculated from the resulting distribution according to Eq. (5), was 0.85 μs. The value obtained for the corresponding hydrogen case from Eq. (6) is 0.89 μs. The effect of the presence of the oxygen and the energy dependence of the hydrogen cross section is thus a shortening of the slowing-down time of 0.04 μs. The shape of the distribution curve agrees well with Eq. (3), and a least squares fit of this function to the data from the Monte Carlo calculation resulted in a value for Σ_s of 1.38 cm^{-1}, corresponding to an "effective hydrogen cross section" in the energy range considered of 20.6 barns.

7. Discussion of the results

a) Comparison with the theory for the infinite medium

Since the recorded curves show an apparent space dependence, a direct comparison with Eq. (1) can not be made. It would require an integration of curves measured at all places in the tank, since the energy spectrum of the fast neutron source depends on the angle of emission. However, as is seen in Fig. 3, the calculated curve for the infinite medium (the full line curve) reproduces the shape of the experimental curve at the spatial region, where most neutrons are expected to pass 1.46 eV, very well. Considering the correction for time shift, which should move the measured curve slightly towards longer times, and the correction according to the Monte Carlo calculations, which would

shift the calculated curve towards shorter times, this agreement can be considered as a rather good verification of Eq. (1).

It is very difficult to make an integrating measurement by distributing indium in the whole tank and measure with only one gamma ray detector, since the spatial and directional efficiency dependence of the detector will introduce a weighting factor which is very difficult to analyze and correct for. Therefore, it would not be surprising if the measurement under these conditions at a distance of 12 cm from the source showed deviations from the infinite medium curve. The result was, however, a curve, which gave a good fit to Eq. (12) and a time for the maximum of 0.90 μs. This differs rather little from the infinite medium value, which should, according to the Monte Carlo calculation, be about 0.86 μs.

b. Comparison with the space dependent theory

The parameter, which will be compared with the predictions from theory, is the time for the maximum neutron density. The results might also be described by the time integral of the curves at each position and compared with age calculations, but this kind of study can be performed with much higher precision by the use of a monoenergetic isotropic radioactive source and detection with activation technique [24]. The position of the maximum was found by least squares fits to the experimental data of Eq. (16), to which was added an exponential factor for absorption. The time value will then apply to the case of no absorption. The results are shown in Table I. The radial position corresponding to the source-container distance is in each case estimated from the relative intensities and the shapes of the containers. The error in the determination of the time is less than 1 %. The time shift correction has been taken as + 0.02 μs. This value was found through extrapolation to zero absorption in the measurements shown in Fig. 3. The peaks occur at the times 0.89, 0.84, and 0.67 μs. This dependence on the concentration is smaller than the calculated value, due to the different conditions in the two cases. To this correction has also been added a correction of + 0.02 μs, which was found in test fits to the calculated reaction rate curves with and without the two higher resonance included.

In the paper by Claesson [4], an equation is given for the space and time dependent neutron density in the eV region after slowing down from high energies. The final formula is rather space-consuming and

will not be cited here. A P_1-approximation has been used. In [4] results were given for two cases. Numerical results for one of these are given in Table II. The chosen case is the one where the time derivative of the first moment has been disregarded, since the inclusion of this term seemed to give too strong space-dependence near the source. For each chosen value of source energy, E_o, and position, r, the complete curves were calculated, but only $t_{max.n}$ and the numerical value of the neutron density at this time are reproduced. $t_{max.n}$ is seen to depend very much on the distance from the source for a source energy of 0.1 MeV. For 2 MeV the variation is much smaller. The paper by Dyad'kin and Batalina [3] gives also a formula, which should be applicable to these measurements, and $t_{max.n}$ as a function of the distance to the source has been calculated for a source energy of 1 MeV.

The results of the measurements have been plotted in Fig. 7 and the theoretical calculations mentioned above have been included. Error bars have been given for the experimental points, indicating the uncertainty of the determination of the spatial point representative for the time value.

The behaviour of the neutron distributions at different places will be dominated by neutrons slowed down from different source energies. According to Table II, the neutrons starting from 0.1 MeV contribute most at r = 0, whereas at r = 20 cm, the neutrons with a source energy of 2.0 MeV are in majority and the number that started at 0.1 MeV are negligible. Thus, we cannot exactly compare the experimental results with only one of the Claesson curves in Fig. 7, but the comparison should be done, keeping the source spectrum in mind. It would, in principle, be possible to calculate the expected time-dependent density curves at each point by including the source spectrum. The cost of such a calculation would be quite high, and the result would not include the anisotropy of the source. It is evident, however, that the space-dependence obtained experimentally for $t_{max.n}$ is rather well reproduced by the calculations of Claesson. Around 5 cm all curves yield the same $t_{max.n}$, and when proceeding outwards, the comparison shall be made with curves corresponding to increasing source energy. The physical meaning behind is, of course, that during the first collisions, which are the most important ones for the establishment of the spatial distribution, the high energy

neutrons diffuse longer because of the decrease of the hydrogen scattering cross section with increasing energy.

The curve calculated according to Dyad'kin and Batalina on the other hand, does not reproduce the experiment. The time values are too high. The reason is probably the use of concepts and parameters from age theory, and the theory can be expected to work better for slowing-down in heavier moderators or for mixtures with low hydrogen percentage.

A more exact comparison between theory and experiment for the process studied in this work would require improvements of the experimental conditions. In our case, less than 1 % of the available accelerator current was efficiently used, since an external pulser rejected machine pulses during the time neutrons underwent moderation and absorption. It may be possible to use other techniques to raise the efficiency. Then thinner targets could be used and almost monoenergetic neutrons could be obtained. Two possible methods have been contemplated. One would be to accept target pulses at a higher rate and apply correlation technique to extract the information wanted; the other, to switch the accelerator pulses presently wasted into a storage ring which were emptied at a rate suitable for the experiment. Both methods would, unfortunately, be expensive.

8. Conclusions

The application of the method of time analysis of capture gamma rays from indium in a dilute solution has confirmed the validity of the theory of Marshak for the time-dependent neutron density in a hydrogenous medium as far as this can be done, using a pulsed point neutron source of presently available intensity. The theoretical analysis and the experiments have displayed the importance of using low spectrum indicator concentrations in order to avoid perturbations in the time distributions. The space-dependence of the time for the maximum density of neutrons at 1.46 eV is in accord with the predictions from the P_1-calculations by Claesson.

9. Acknowledgements

The author wished to express his gratitude to Professor N.G. Sjöstrand for the suggestion of slowing-down studies, which has led to

this work, and for many stimulating discussions. The interest shown by Dr. A. Claesson in these studies and his theoretical work has been very encouraging. The help with numerical calculations by fil.kand. G. Näslund is also gratefully acknowledged. The author is also indebted to fil.kand. T. Högberg for making available the Monte Carlo calculations.

References

1. ORNSTEIN, L S and UHLENBECK, G E,
Physica 4 (1937) 478.

2. MARSHAK, R E,
Rev. Mod. Phys. 19 (1947) 185.

3. DYAD'KIN, I G and BATALINA, E P,
Atomnaya Energiya 10 (1961) 5; React. Sci. Techn. 16 (1962) 103.

4. CLAESSON, A,
1963 (AE-129).

5. VON DARDEL, G F,
Trans. Roy. Inst. Technol., Stockholm (1954) No. 75.

6. HAYNAM, G E and CROUCH, M F,
Nucl. Sci. Eng. 2 (1957) 626.

7. KRIEGER, T J and FEDERIGHI, F D,
Trans. Am. Nucl. Soc. 2 (1959):2, 102.

8. AMALDI, E,
The production and slowing down of neutrons. Handbuch der Physik 38/2, 1959, Berl., Springer. p. 246.

9. MICHAUDON, A,
React. Sci. Techn. 17 (1963) 165.

10. CROUCH, M F,
Nucl. Sci. Eng. 2 (1957) 631.

11. HOLZER, F and CROUCH, M F,
Nucl. Sci. Eng. 6 (1959) 545.

12. ENGELMANN, P,
Nukleonik 1 (1958) 125.

13. BECKURTS, K H and WIRTZ, K,
Neutron Physics 1964, Berl. Springer. p. 354.

14. MÖLLER, E and SJÖSTRAND, N G,
1962 (BNL 719 (C-32)) 966.

15. MÖLLER, E and SJÖSTRAND, N G,
Nucl. Sci. Eng. 15 (1963) 221.

16. MÖLLER, E and SJÖSTRAND, N G,
Arkiv Fysik 27 (1964) 501.

17. SHUKLA, A P and WALTNER, A,
Nukleonik 6 (1964) 1.

18. PROFIO, A E and ECKARD, J D,
Nucl. Sci. Eng. 19 (1964) 321.

19. DeJUREN, J A,
Nucl. Sci. Eng. 9 (1961) 408.

20. GROSSHÖG, G,
Arkiv Fysik 27 (1964) 215.

21. HUGHES, D J and SCHWARZ, R B,
2 ed. 1958 (BNL 325).

22. WESTCOTT, C H,
3 ed. 1960 (AECL-1101).

23. HÖGBERG, T, LJUNGGREN, S and PERSSON, P E,
1964 AB Atomenergi, Internal report (RFR-288).

24. FOSTER, D G, Jr.,
Nucl. Sci. Eng. 8 (1960) 148.

Table I. The measured time for the maximum neutron density as a function of the distance from the source.

x, cm	r, cm	t_{max}, μs	t_{max}, corr., μs
1.5	4.5	0.83	0.87
5.5	7.5	0.89	0.93
9.5	11.5	0.96	1.00
7.0	11.0	0.94	0.98
11.0	16.0	0.96	1.00
13.0	18.0	0.98	1.02

Table II. Time for maximum neutron density according to Claesson's formula.

r, cm	E_o, MeV	t_{max}, μs	$n(t_{max})$
0	0.1	0.68	$0.102 \cdot 10^{-8}$
	0.5	0.72	$0.619 \cdot 10^{-9}$
	1.0	0.75	$0.466 \cdot 10^{-9}$
	2.0	0.77	$0.342 \cdot 10^{-9}$
5	0.1	0.86	$0.318 \cdot 10^{-9}$
	0.5	0.85	$0.261 \cdot 10^{-9}$
	1.0	0.85	$0.221 \cdot 10^{-9}$
	2.0	0.84	$0.177 \cdot 10^{-9}$
10	0.1	1.15	$0.236 \cdot 10^{-10}$
	0.5	1.04	$0.336 \cdot 10^{-10}$
	1.0	0.99	$0.372 \cdot 10^{-10}$
	2.0	0.96	$0.378 \cdot 10^{-10}$
15	0.1	1.48	$0.880 \cdot 10^{-12}$
	0.5	1.18	$0.254 \cdot 10^{-11}$
	1.0	1.06	$0.430 \cdot 10^{-11}$
	2.0	1.01	$0.637 \cdot 10^{-11}$
20	0.1	1.77	$0.217 \cdot 10^{-13}$
	0.5	1.22	$0.164 \cdot 10^{-12}$
	1.0	1.08	$0.514 \cdot 10^{-12}$
	2.0	1.01	$0.122 \cdot 10^{-11}$

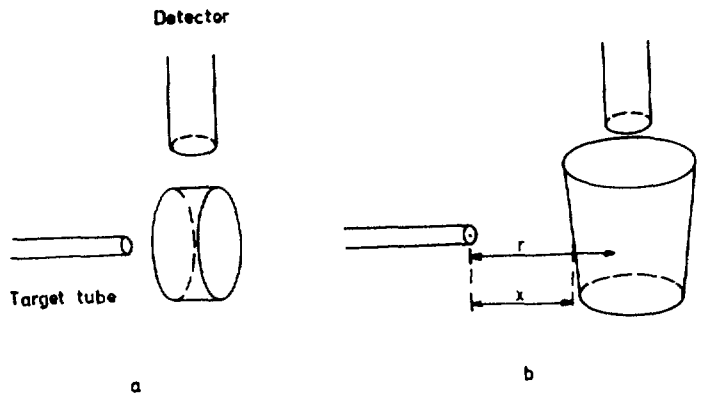

Fig. 1

Geometrical arrangement of the target tube, indicator container and gamma ray detector in the moderator.

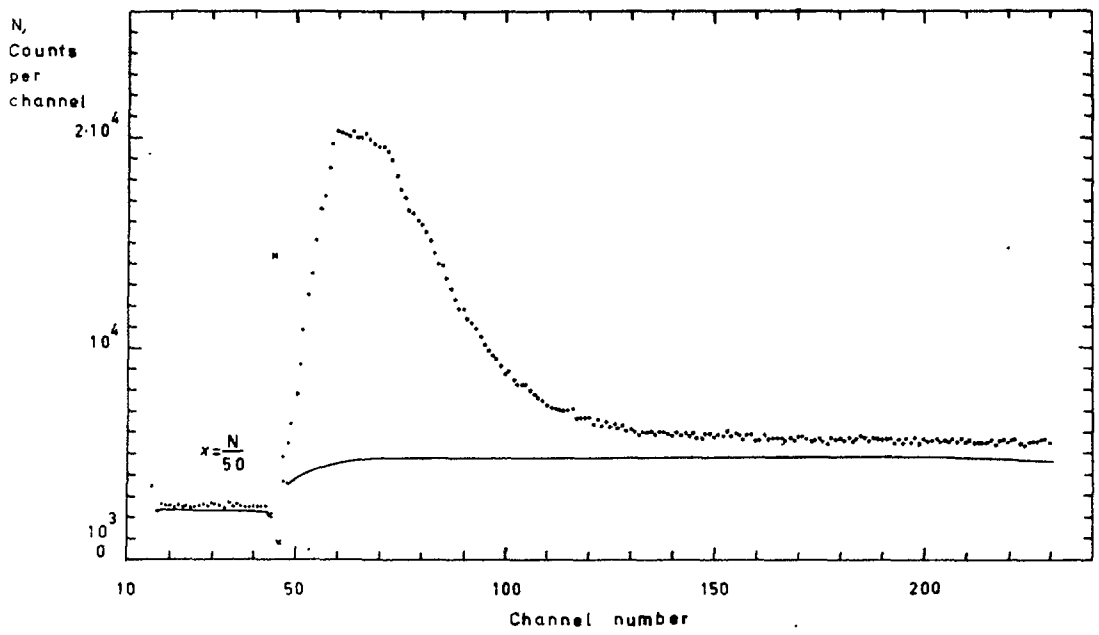

Fig. 2

Time analyzer records from a measurement with (dots) and without (smoothed curve) the indicator pot. The channel width is 0.0417 μs, and injection takes place at channel 45.

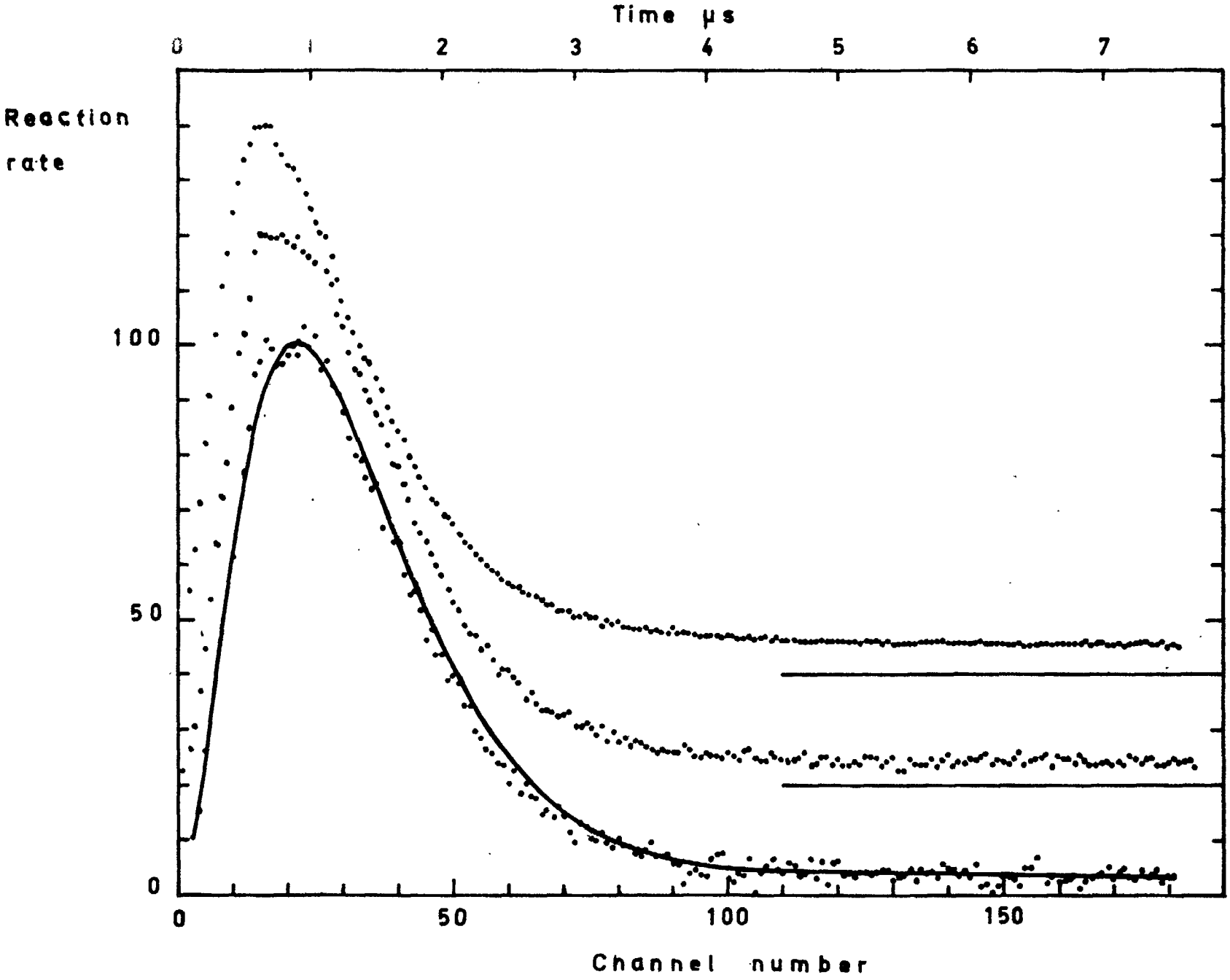

Fig. 3

Results of measurements at a source-container distance of 3 cm with three concentrations of indium. For clarity, the curves have been displaced relative to each other. The figure illustrates the shift towards shorter times with increasing concentration (upper curves). Channel width 0.0417 μs.

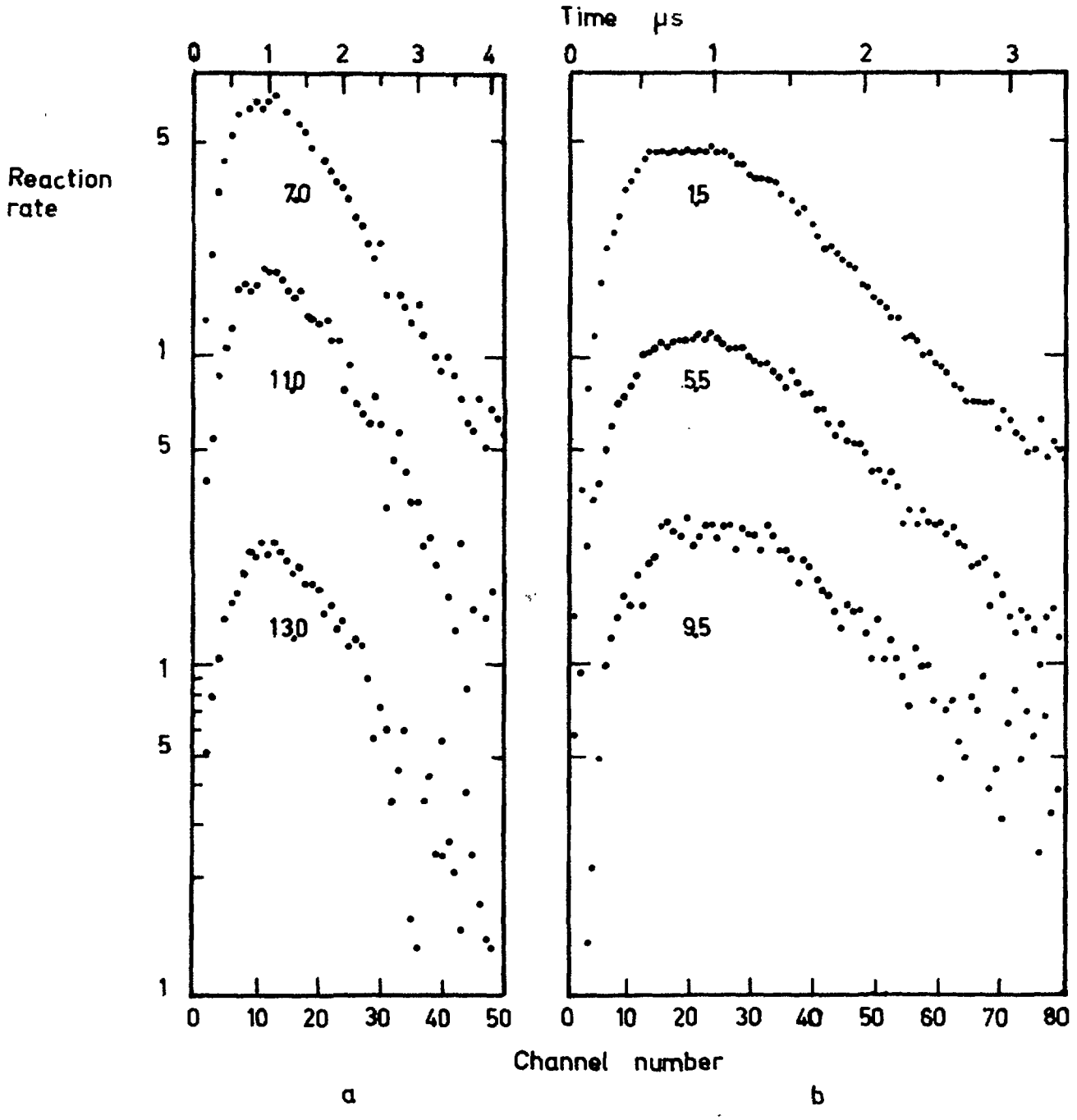

Fig. 4

Indium measurements at different distances with the weakest solution. In a) the channel width is 0.0834 μs and the container volume 1.5 l. In b) corresponding figures are 0.0417 μs and 0.4 l.

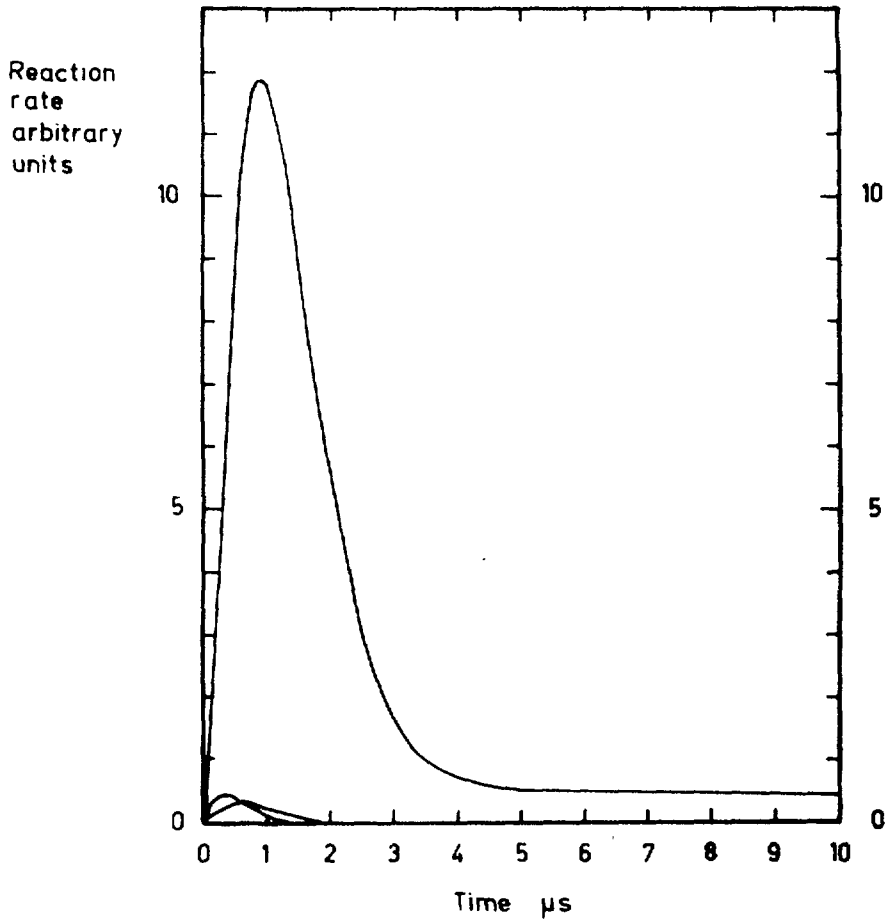

Fig. 5

Calculated reaction rate curves for indium and time-dependent flux according to Marshak. For an assumed mean free path of 0.75 cm, the peak for the 1.46 eV resonance appears at 0.90 μs, for 3.86 eV at 0.55 μs, and for 9.10 eV at 0.35 μs.

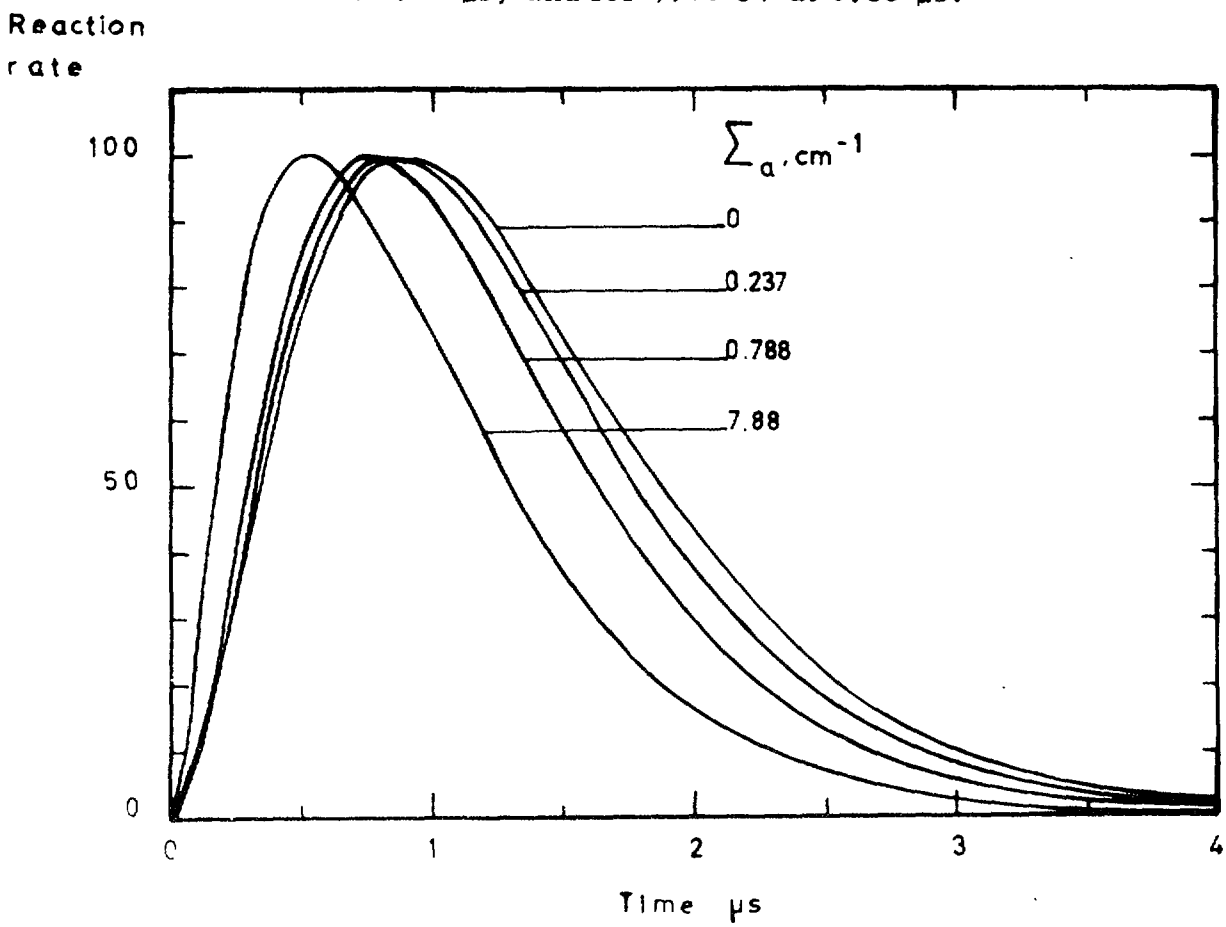

Fig. 6

Calculated reaction rate curves for indicators of different absorption cross section at 1.46 eV and a flux according to Marshak.

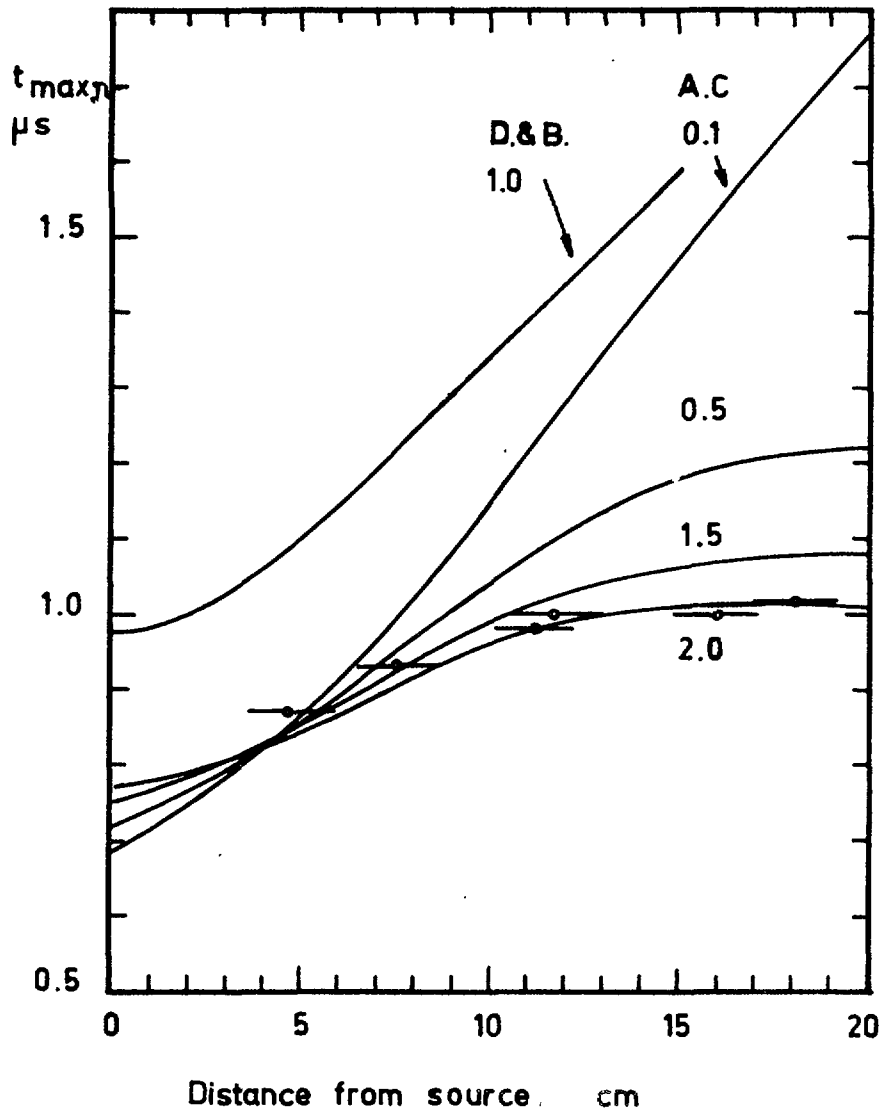

Fig. 7

Experimental results of $t_{max.n}$ versus radius, and calculations according to the theories of Claesson (A.C., for source energies 0.1 - 2.0 MeV) and Dyad'kin and Batalina (D.&B., 1.0 MeV).

LIST OF PUBLISHED AE-REPORTS

1—130. (See the back cover earlier reports.)

132. A neutron rem counter. By I. Ö. Andersson and J. Braun. 1964. 14 p. Sw. cr. 8:—.
133. Studies of water by scattering of slow neutrons. By K. Sköld, E. Pilcher and K. E. Larsson. 1964. 17 p. Sw. cr. 8:—.
134. The amounts of As, Au, Br, Cu, Fe, Mo, Se, and Zn in normal and uraemic human whole blood. A comparison by means neutron activation analysis. By D. Brune, K. Samsahl and P. O. Wester. 1964. 10 p. Sw. cr. 8:—.
135. A Monte Carlo method för the analysis of gamma radiation transport from distributed sources in laminated shields. By M. Leimdörfer. 1964. 28 p. Sw. cr. 8:—.
136. Ejection of uranium atoms from UO_2 by fission fragments. By G. Nilsson. 1964. 38 p. Sw. cr. 8:—.
137. Personell neutron monitoring at AB Atomenergi. By S. Hagsgård and C.-O. Widell. 1964. 11 p. Sw. cr. 8:—.
138. Radiation induced precipitation in iron. By B. Solly. 1964. 8 p. Sw. cr. 8:—.
139. Angular distributions of neutrons from (p, n)-reactions in some mirror nuclei. By L. G. Strömberg, T. Wiedling and B. Holmqvist. 1964. 28 p. Sw. cr. 8:—.
140. An extended Greuling-Goertzel approximation with a P_n -approximation in the angular dependence. By R. Håkansson. 1964. 21 p. Sw. cr. 8:—.
141. Heat transfer and pressure drop with rough surfaces, a literature survey. By A. Bhattachayya. 1964. 78 p. Sw. cr. 8:—.
142. Radiolysis of aqueous benzene solutions. By H. Christensen. 1964. 50 p. Sw. cr. 8:—.
143. Cross section measurements for some elements suited as thermal spectrum indicators: Cd, Sm, Gd and Lu. By E. Sokolowski, H. Pekarek and E. Jonsson. 1964. 27 p. Sw. cr. 8:—.
144. A direction sensitive fast neutron monitor. By B. Antolkovic, B. Holmqvist and T. Wiedling. 1964. 14 p. Sw. cr. 8:—.
145. A user's manual for the NRN shield design method. By L. Hjärne. 1964. 107 p. Sw. cr. 10:—.
146. Concentration of 24 trace elements in human heart tissue determined by neutron activation analysis. By P. O. Wester. 1964. 33 p. Sw. cr. 8:—.
147. Report on the personnel Dosimetry at AB Atomenergi during 1963. By K.-A. Edvardsson and S. Hagsgård. 1964. 16 p. Sw. cr. 8:—.
148. A calculation of the angular moments of the kernel for a monatomic gos scatterer. By R. Håkansson. 1964. 16 p. Sw. cr. 8:—.
149. An anion-exchange method for the separation of P-32 activity in neutron-irradited biological material. By K. Samsahl. 1964. 10 p. Sw. cr 8:—.
150. Inelastic neutron scattering cross sections of Cu^{63} and Cu^{65} in the energy region 0.7 to 1.4 MeV. By B. Holmqvist and T. Wiedling. 1964. 30 p. Sw. cr. 8:—.
151. Determination of magnesium in needle biopsy samples of muscle tissue by means of neutron activation analysis. By D. Brune and H. E. Sjöberg. 1964. 8 p. Sw. cr. 8:—.
152. Absolute El transition probabilities in the dofermed nuclei Yb^{177} and Hf^{179}. By Sven G. Malmskog. 1964. 21 p. Sw. cr. 8:—.
153. Measurements of burnout conditions for flow of boiling water in vertical 3-rod and 7-rod clusters. By K. M. Becker, G. Hernborg and J. E. Flinta. 1964. 54 p. Sw. cr. 8:—.
154. Integral parameters of the thermal neutron scattering law. By S. N. Purohit. 1964. 48 p. Sw. cr. 8:—.
155. Tests of neutron spectrum calculations with the help of foil measurments in a D_2O and in an H_2O-moderated reactor and in reactor shields of concrete and iron. By R. Nilsson and E. Aalto. 1964. 23 p. Sw. cr. 8:—.
156. Hydrodynamic instability and dynamic burnout in natural circulation two-phase flow. An experimental and theoretical study. By K. M. Becker. S. Jahnberg, I. Haga, P. T. Hansson and R. P. Mathisen. 1964. 41 p. Sw. cr. 8:—.
157. Measurements of neutron and gamma attenuation in massive laminated shields of concrete and a study of the accuracy of some methods of calculation. By E. Aalto and R. Nilsson. 1964. 110 p. Sw. cr. 10:—.
158. A study of the angular distributions of neutrons from the Be^9 (p,n) B^9 reaction at low proton energies. By. B. Antolkovic', B. Holmqvist and T. Wiedling. 1964. 19 p. Sw. cr. 8:—.
159. A simple apparatus for fast ion exchange separations. By K. Samsahl. 1964. 15 p. Sw. cr. 8:—.
160. Measurements af the Fe^{54} (n, p) Mn^{54} reaction cross section in the neutron energy range 2.3—3.8 MeV. By A. Lauber and S. Malmskog. 1964. 13 p. Sw. cr. 8:—.
161. Comparisons of measured and calculated neutron fluxes in laminated iron and heavy water. By. E. Aalto. 1964. 15. p. Sw. cr. 8:—.
162. A needle-type p-i-n junction semiconductor detector for in-vivo measurement of beta tracer activity. By A. Lauber and B. Rosencrantz. 1964. 12 p. Sw. cr. 8:—.
163. Flame spectro photometric determination of strontium in water and biological material. By G. Jönsson. 1964. 12 p. Sw. cr. 8:—.
164. The solution of a velocity-dependent slowing-down problem using case's eigenfunction expansion. By A. Claesson. 1964. 16 p. Sw. cr. 8:—.
165. Measurements of the effects of spacers on the burnout conditions for flow of boiling water in a vertical annulus and a vertical 7-rod cluster. By K. M. Becker and G. Hernberg. 1964. 15 p. Sw. cr. 8:—.
166. The transmission of thermal and fast neutrons in air filled annular ducts through slabs of iron and heavy water. By J. Nilsson and R. Sandlin. 1964. 33 p. Sw. cr. 8:—.
167. The radio-thermoluminescense of $CaSO_4$: Sm and its use in dosimetry. By B. Bjärngard. 1964. 31 p. Sw. cr. 8:—.
168. A fast radiochemical method for the determination of some essential trace elements in biology and medicine. By K. Samsahl. 1964. 12 p. Sw. cr. 8:—.
169. Concentration of 17 elements in subcellular fractions of beef heart tissue determined by neutron activation analysis. By P. O. Wester. 1964. 29 p. Sw. cr. 8:—.
170. Formation of nitrogen-13, fluorine-17, and fluorine-18 in reactor-irradiated H_2O and D_2O and applications to activation analysis and fast neutron flux monitoring. By L. Hammar and S. Forsén. 1964. 25 p. Sw. cr. 8:—.
171. Measurements on background and fall-out radioactivity in samples from the Baltic bay of Tvären, 1957—1963. By P. O. Agnedal. 1965. 48 p. Sw. cr. 8:—.
172. Recoil reactions in neutron-activation analysis. By D. Brune. 1965. 24 p. Sw. cr. 8:—.
173. A parametric study of a constant-Mach-number MHD generator with nuclear ionization. By J. Braun. 1965. 23 p. Sw. cr. 8:—.
174. Improvements in applied gamma-ray spectrometry with germanium semiconductor dector. By D. Brune, J. Dubois and S. Hellström. 1965. 17 p. Sw. cr. 8:—.
175. Analysis of linear MHD power generators. By E. A. Witalis. 1965. 37 p. Sw. cr. 8:—.
176. Effect of buoyancy on forced convection heat transfer in vertical channels — a literature survey. By A. Bhattacharyya. 1965. 27 p. Sw. cr. 8:—.
177. Burnout data for flow of boiling water in vertical round ducts, annuli and rod clusters. By K. M. Becker, G. Hernborg, M. Bode and O. Eriksson. 1965. 109 p. Sw. cr. 8:—.
178. An analytical and experimental study of burnout conditions in vertical round ducts. By K. M. Becker. 1965. 161 p. Sw. cr. 8:—.
179. Hindered El transitions in Eu^{155} and Tb^{161}. By S. G. Malmskog. 1965. 19 p. Sw. cr. 8:—.
180. Photomultiplier tubes for low level Cerenkov detectors. By O. Strindehag. 1965. 25 p. Sw. cr. 8:—.
181. Studies of the fission integrals of U235 and Pu239 with cadmium and boron filters. By E. Hellstrand. 1965. 32 p. Sw. cr. 8:—.
182. The handling of liquid waste at the research station af Studsvik, Sweden. By S. Lindhe and P. Linder. 1965. 18 p. Sw. cr. 8:—.
183. Mechanical and instrumental experiences from the erection, commissioning and operation of a small pilot plant for development work on aqueous reprocessing of nuclear fuels. By K. Jönsson. 1965. 21 p. Sw. cr. 8:—.
184. Energy dependent removal cross-sections in fast neutron shielding theory. By H. Grönroos. 1965. 75 p. Sw. cr. 8:—.
185. A new method for predicting the penetration and slowing-down of neutrons in reactor shields. By L. Hjärne and M. Leimdörfer. 1965. 21 p. Sw. cr. 8:—.
186. An electron microscope study of the thermal neutron induced loss in high temperature tensile ductility of Nb stabilized austenitic steels. By R. B. Roy. 1965. 15 p. Sw. cr. 8:—.
187. The non-destructive determination of burn-up means of the Pr-144 2.18 MeV gamma activity. By R. S. Forsyth and W. H. Blackadder. 1965. 22 p. Sw. cr. 8:—.
188. Trace elements in human myocardial infarction determined by neutron activation analysis. By P. O. Wester. 1965. 34 p. Sw. cr. 8:—.
189. An electromagnet for precession of the polarization of fast-neutrons. By O. Aspelund, J. Bäckman and G. Trumpy. 1965. 28 p. Sw. cr. 8:—.
190. On the use of importance sampling in particle transport problems. By B. Eriksson. 1965. 27 p. Sw. cr. 8:—.
191. Trace elements in the conductive tissue of beef heart determined by neutron activation analysis. By P. O. Wester. 1965. 19 p. Sw. cr. 8:—.
192. Radiolysis of aqueous benzene solutions in the presence of inorganic oxides. By H. Christensen. 12 p. 1965. Sw. cr. 8:—.
193. Radiolysis of aqueous benzene solutions at higher temperatures. By H. Christensen. 1965. 14 p. Sw. cr. 8:—.
194. Theoretical work for the fast zero-power reactor FR-0. By H. Häggblom. 1965. 46 p. Sw. cr. 8:—.
195. Experimental studies on assemblies 1 and 2 of the fast reactor FR0. Part 1. By T. L. Andersson, E. Hellstrand, S-O. Londen and L. I. Tirén. 1965. 45 p. Sw. cr. 8:—.
196. Measured and predicted variations in fast neutron spectrum when penetrating laminated Fe-D_2O. By E. Aalto, R. Sandlin and R. Fräki. 1965. 20 p. Sw. cr. 8:—.
197. Measured and predicted variations in fast neutron spectrum in massive shields of water and concrete. By E. Aalto, R. Fräki and R. Sandlin. 1965. 27 p. Sw. cr. 8:—.
198. Measured and predicted neutron fluxes in, and leakage through, a configuration of perforated Fe plates in D_2O. By E. Aalto. 1965. 23 p. Sw. cr. 8:—.
199. Mixed convection heat transfer on the outside of a vertical cylinder. By A. Bhattacharyya. 1965. 42 p. Sw. cr. 8:—.
200. An experimental study of natural circulation in a loop with parallel flow test sections. By R. P. Mathisen and O. Eklind. 1965. 47 p. Sw. cr. 8:—.
201. Heat transfer analogies. By A. Bhattacharyya. 1965. 55 p. Sw. cr. 8:—.
202. A study of the "384" KeV complex gamma emission from plutonium-239. By R. S. Forsyth and N. Ronqvist. 1965. 14 p. Sw. cr. 8:—.
203. A scintillometer assembly for geological survey. By E. Dissing and O. Landström. 1965. 16 p. Sw. cr. 8:—.
204. Neutron-activation analysis of natural water applied to hydrogeology. By O. Landström and C. G. Wenner. 1965. 28 p. Sw. cr. 8:—.
205. Systematics of absolute gamma ray transition probabilities in deformed odd-A nuclei. By S. G. Malmskog. 1965. 60 p. Sw. cr. 8:—.
206. Radiation induced removal of stacking faults in quenched aluminium. By U. Bergenlid. 1965. 11 p. Sw. cr. 8:—.
207. Experimental studies on assemblies 1 and 2 of the fast reactor FR0. Part 2. By E. Hellstrand, T. L. Andersson, B. Brunfelter, J. Kockum, S-O. Londen and L. I. Tirén. 1965. 50 p. Sw. cr. 8:—.
208. Measurement of the neutron slowing-down time distribution at 1.46 eV and its space dependence in water. By E. Möller. 1965. 29. p. Sw. cr. 8:—.

Förteckning över publicerade AES-rapporter

1. Analys medelst gamma-spektrometri. Av D. Brune. 1961. 10 s. Kr 6:—.
2. Bestrålningsförändringar och neutronatmosfär i reaktortrycktankar — några synpunkter. Av M. Grounes. 1962. 33 s. Kr 6:—.
3. Studium av sträckgränsen i mjukt stål. Av G. Östberg och R. Attermo. 1963. 17 s. Kr 6:—.
4. Teknisk upphandling inom reaktorområdet. Av Erik Jonson. 1963. 64 s. Kr 8:—.
5. Agesta Kraftvärmeverk. Sammanställning av tekniska data, beskrivningar m. m. för reaktordelen. Av B. Lilliehöök. 1964. 336 s. Kr 15:—.

Additional copies available at the library of AB Atomenergi, Studsvik, Nyköping, Sweden. Transparent microcards of the reports are obtainable through the International Documentation Center, Tumba, Sweden.

EOS-tryckerierna, Stockholm 1965